# Lipid–cholesterol interactions in the $P_{\beta'}$ phase

## Application of a statistical mechanical model

H. L. Scott and W. Scott McCullough

Department of Physics, Oklahoma State University, Stillwater, Oklahoma 74078-0444 USA

ABSTRACT We describe a statistical mechanical model for lipid–cholesterol mixtures in the $P_{\beta'}$ (ripple) phase of lipid bilayers. The model is a simple extension of an earlier model for the ripple phase in pure lipid bilayers. The extension consists of adding a degree of freedom to allow for the occupation of underlying lattice sites by cholesterol molecules, and adding a lipid–cholesterol interaction term to the model Hamiltonian. The interaction term was constructed based on numerical calculations of lipid–cholesterol energies for several different packing juxtapositions of the two molecules. Other than the lipid–cholesterol interactions, the extended model uses the same parameter set as the earlier model, so that comparison of the properties of the extended model with experimental data serves as a test of the validity of the original model. Properties of the model were calculated using the Monte Carlo method. Results are displayed as snapshots of the ripple configurations at different cholesterol concentrations. The spacing of the ripples increases with increasing cholesterol concentration and the rate of increase compares very well with experimental data. The success of this model supports the conclusion drawn earlier that frustration arising from anisotropic packing interactions is responsible for the ripple phase in lipid bilayers. In the extended model these packing interactions are responsible for the selective partitioning of cholesterol in the regions between the ripples.

## INTRODUCTION

Cholesterol is an important ingredient in animal cell membranes. Because the cholesterol molecular structure is simple and the molecule itself is relatively small, the influence it exerts in biomembranes should be primarily limited to *physical* interactions with other membrane molecules. For this reason there has been a great deal of research devoted to understanding the thermophysical properties of model membranes containing controlled concentrations of cholesterol (1, 2). While much of this effort has been directed towards interactions between cholesterol and lipids in the fluid lipid phase, or near the main lipid phase transition (3), less is known about the effect of cholesterol on the $P_{\beta'}$, or ripple phase exhibited by a large class of phospholipid bilayers.

The first detailed experimental study of the effect of cholesterol on the structure of the $P_{\beta'}$ phase of lipid bilayers was carried out by Copeland and McConnell (4). Using freeze-fracture microscopy they found that the primary ripple repeat distance increased approximately linearly with increasing cholesterol concentration up to about 15 mol% cholesterol. Between 15 mol% and 20 mol% cholesterol the ripple repeat distance increased more rapidly, and, above 20 mol%, the ripple phase disappeared altogether. Freeze-fracture studies by Hicks et al. (5) have confirmed the earlier experiments and have provided quantitative measures of the change in ripple repeat distance with cholesterol concentration. Small angle neutron scattering experiments (6) have also confirmed an increase in repeat distance with cholesterol concentration.

The increase in ripple repeat distance with increasing cholesterol concentration has been interpreted in all cases as a consequence of preferential location of cholesterol in the "troughs" or "peaks" of the ripples (4–6). This interpretation is supported by flourescence photobleaching recovery measurements of Schneider et al. (7). These experiments found two independent diffusion pathways which differed by two orders of magnitude in diffusion rate. The faster diffusion occurred parallel to the ripple corrugations and may be due to greater molecular disorder, mainly in the form of packing defects, in these regions. An additional thermodynamic structure, called the $P'_{\beta'}$ phase was found in neutron scattering data and was attributed to cholesterol clustering (at sufficiently high mol%) within the regions of increased disorder (6).

In recent years a wide variety of theoretical models for the $P_{\beta'}$ phase have been proposed (for a review, see reference [8]). These models range in scope from continuum Landau Theories (9–13) to lattice statistical mechanical models (14–17). While most of the proposed models contain modulated phases which are associated with the experimental $P_{\beta'}$ phase, to date none have been extended to describe the effect of cholesterol on this phase. Such an extension of a theoretical model, without additional phenomenological modifications, tests the ability of the model to predict *independent* properties which are observed experimentally.

In this paper we describe an extension of a statistical mechanical model for the $P_{\beta'}$ phase to include cholesterol. We show that cholesterol can be added to the model in a very simple and transparent manner. We then show that the properties of the extended model, as determined by Monte Carlo simulation, agree well with experimental data. In the next section we describe the model, hereafter referred to as the PS2 model, and we show how the model is modified to include cholesterol.

Address correspondence to Dr. H. L. Scott, Department of Physics, Oklahoma State University, Stillwater, Oklahoma 74078--0444, USA.



0006-3495/93/05/1398/07 $2.00

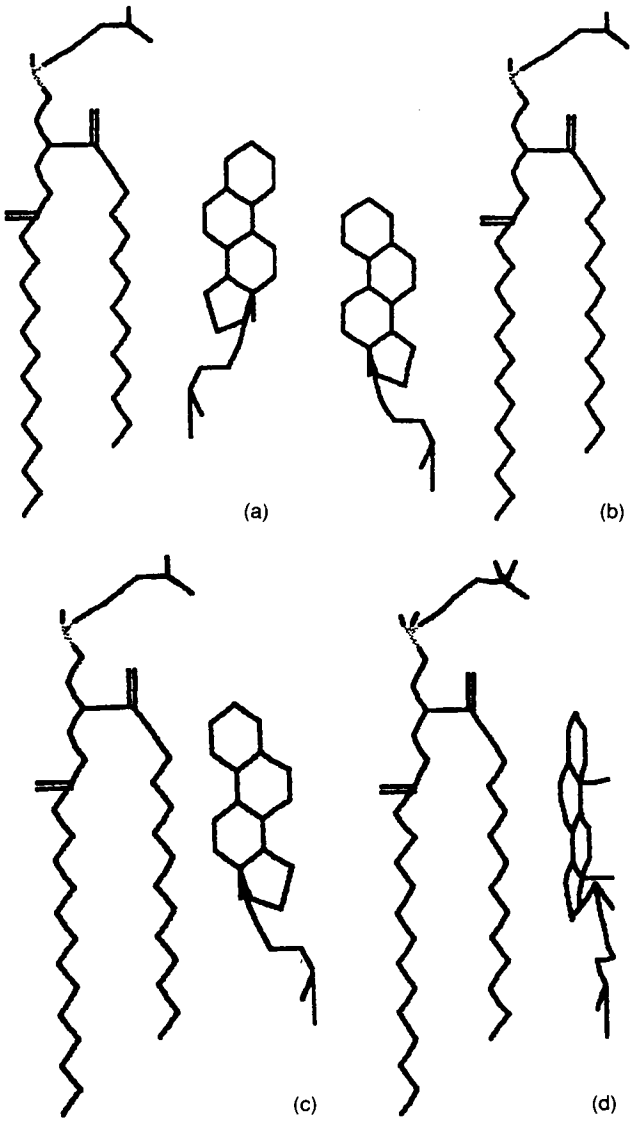


FIGURE 1 Four different conformations of a DMPC molecule and a cholesterol molecule. Energies associated with the conformations were calculated as described in the text and are: (*a*) −7.89 kcal/m; (*b*) −3.79 kcal/m; (*c*) −4.58 kcal/m; (*d*) −5.66 kcal/m.

In subsequent sections the Monte Carlo procedure is described, and results are presented. The final section contains a discussion of the results and a comparison to experimental data.

## MODEL DEFINITION AND METHODS

### The PS2 Model

The basic PS2 model has been defined and analyzed in earlier publications (8, 14, 15, 16). Here we briefly outline the definition in order to show how the model is extended to include cholesterol. Consider a two-dimensional square lattice, representing a plane of reference for a lipid bilayer. Let two lipid molecules, one in each monolayer of the bilayer, occupy each site of the lattice. The lipid molecules are represented as block L-shaped molecules, with the long segment of the L associated with the hydrocarbon chains and the short segment associated with the head group. Each L-shaped molecule is assigned two degrees of freedom; a "height" variable, $n$, and an "orientation" variable, $\sigma$. The height variable is quantized for convenience, $n = 0, \pm 1, \pm 2, \ldots$, and represents the perpendicular displacement of the molecule above or below the plane of reference. The orientation variable $\sigma = \pm 1$ represents the orientation of the lipid head group along one axis in the plane of reference. The basic critical assumptions in this representation of a lipid bilayer *below the main lipid phase transition* are:

- Lipid chain rotameric disordering, while present to a small extent in the $P_{\beta'}$ phase, is not an important factor in the formation of this phase.
- There is a preferred orientation axis for the head groups. This seems to be valid in anhydrous lipid lamellar phases (18), and is also confirmed by preliminary molecular dynamics simulations by H. L. Scott and M. Clark but its status for fully hydrated bilayers is uncertain.
- The two monolayers in the bilayer are, below the main lipid phase transition, very strongly coupled, so that vertical displacements are correlated and no free volume opens up in the bilayer center (it seems obvious that in the ripple phase the two monolayers could not have out-of-phase ripples). This means one need only consider one monolayer.

The Hamiltonian for the PS2 model was originally constructed after a calculation of intermolecular interaction energies for a set of close-packed lipid–lipid pair conformations was done numerically. The construction of an analytic form for the Hamiltonian is not required if one is to simply use Monte Carlo simulations, but is necessary in order to carry out analytical studies of the predicted phases. Since this was the principal goal of our earlier work, the calculated energies were mapped onto a Hamiltonian function which not only correctly reproduced the three lowest calculated interaction energies, but also was an extension of a model known to have incommensurate phases with only nearest neighbor interactions (15, 16). The Hamiltonian is:

$$\mathcal{H} = -\sum_{i}^{N}\sum_{j}^{N}\left(J_0\cos\left\{\frac{2\pi}{p}\left[n_{i+1,j} - n_{i,j} + \frac{\Delta}{2}(\sigma_{i+1,j} + \sigma_{i,j})\right]\right\} + J_1\cos\left[\frac{2\pi}{p}(n_{i,j} - n_{i,j+1})\right] + J_2\sigma_{i,j}\sigma_{i+1,j} + J_3\sigma_{i,j}\sigma_{i,j+1}\right) \quad (1)$$

where $p$ is an integer which was set equal to 5 (this is the lowest value for which a limiting case of the model yields a sufficiently broad incommensurate phase region [14]). The variable $n_{i,j}$ is the height of the molecule at site $(i, j)$, and the variable $\sigma_{i,j} = \pm 1$ denotes the orientation of the

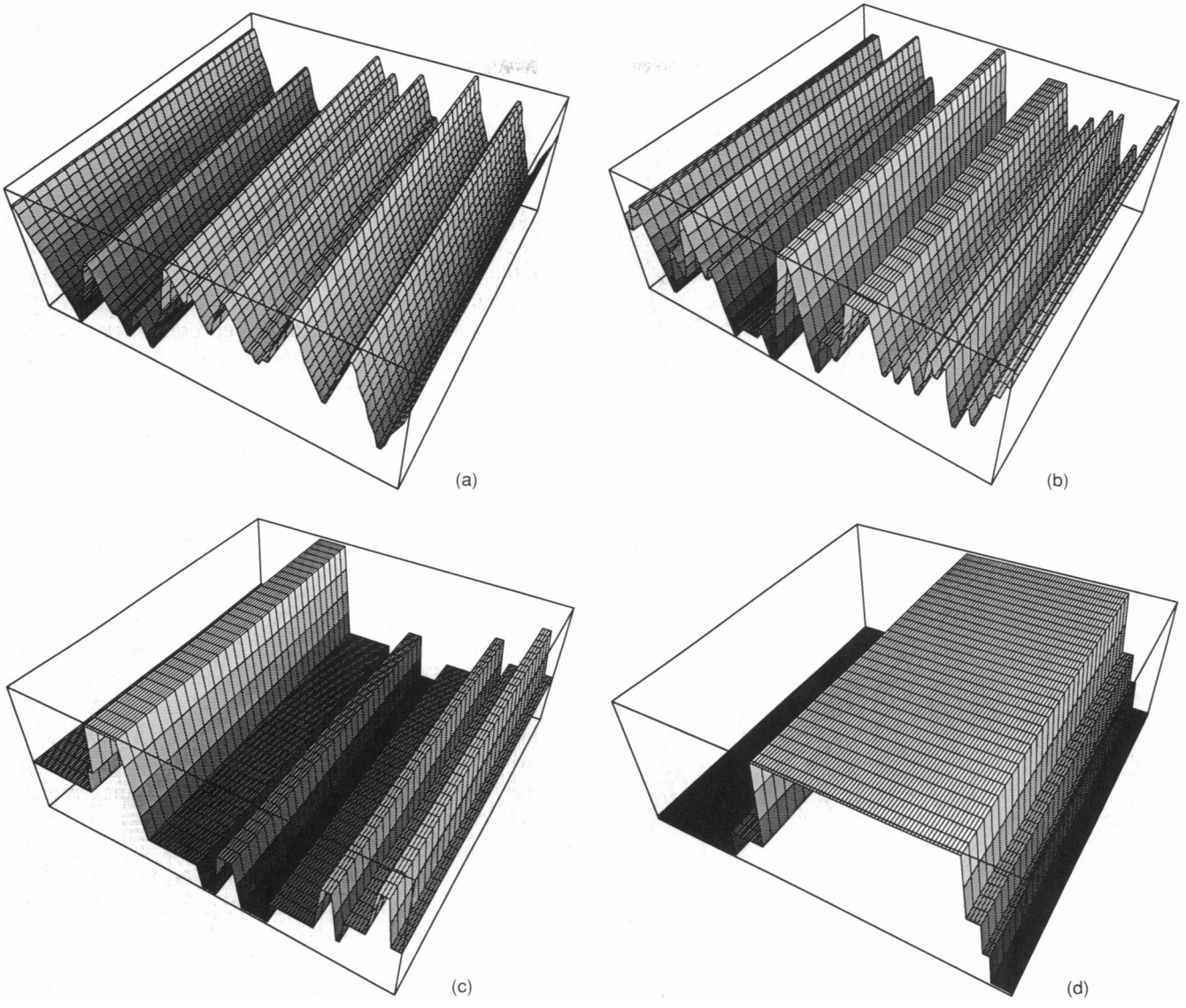


FIGURE 2 Snapshots of vertical molecular positions in final lattice configurations after annealing and running at the final temperature of $k_B T/J_0 = 0.2$ for 50,000 MC steps/site for several cholesterol concentrations. For all cases, $J_4 = 1.45$ kcal/mol. (*a*) cholesterol concentration = 0.00; (*b*) cholesterol concentration = 0.02; (*c*) cholesterol concentration = 0.07; (*d*) cholesterol concentration = 0.10.

head group of the molecule at site $(i, j)$. The sums run over all sites of the lattice. The quantities $J_0$ and $J_2$ are the interaction parameters for nearest neighbor pairs in the ripple direction ($i$), and $J_1$ and $J_3$ are the interaction parameters for nearest neighbor pairs in the $j$-direction.

With $p$ set equal to 5, the values for the interaction parameters $J_0$ and $J_2$, and the parameters and $\Delta$, were chosen so that the three lowest energy pair configurations in the Hamiltonian Eq. 1 agree exactly with the three lowest van der Waals energies for lipid–lipid configurations as determined by independent calculation (14). The parameters $J_1$ and $J_3$ were chosen to reproduce similarly calculated van der Waals energies for the lowest energies of interaction between pairs of DPPC molecules which lie beside each other (not in the direction of anisotropy). The resulting values are: $J_0 = 13.6$ kcal/mol, $J_2 = 0.0971 J_0 = 1.32$ kcal/mol, $J_1 = 1.37 J_0 = 18.6$ kcal/mol, $J_3 = 0.20 J_0 = 2.7$ kcal/mol, and $\Delta = 1.487$.

The parameter set represents states other than the three lowest energy states reasonably well, assigning repulsive energies to conformations in which $\Delta n = 0$ and $\sigma_{i,j} = \sigma_{i+1,j}$, for which there is strong steric repulsion between headgroups at close chain packing. The states for which $\Delta n = 0$ and $\sigma_{i,j} = -\sigma_{i+1,j}$ are both assigned the same energy. This is an assignment based on the calculated energy for the case in which the headgroups point away from each other, but must be taken as an hypothesis for the case in which headgroups point towards each other. The hypothesis is that by some mechanism, such as increased intermolecular separation followed by chain kinking, the lipids in this conformation manage to lower their interaction energy (14).

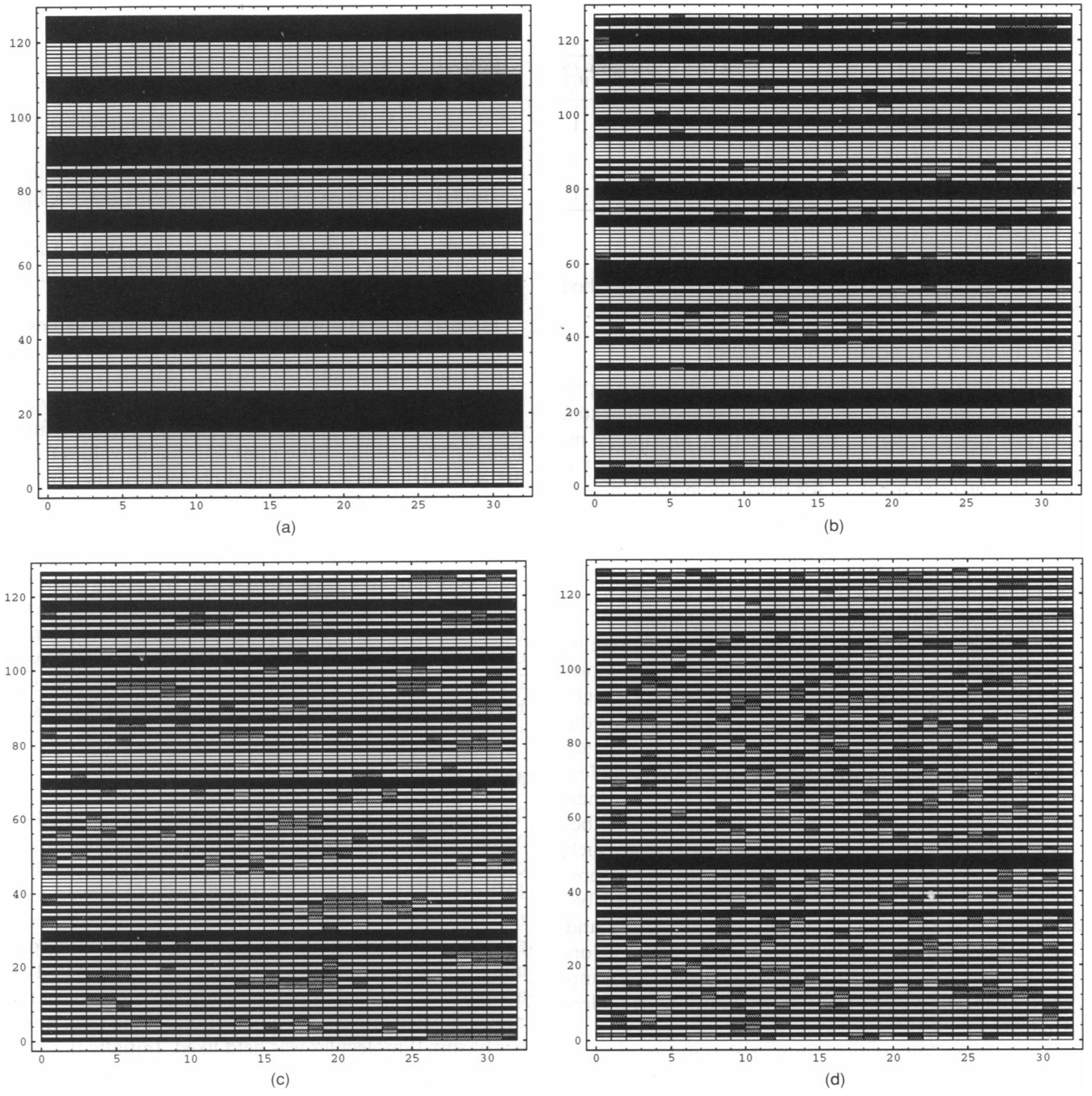


FIGURE 3 Spin density plot showing head group orientations in the same configurations as in Fig. 2. Dark shading indicates $\sigma = +1$, light shading indicates $\sigma = -1$, and gray shading indicates $\sigma = 0$.

Statistical mechanical analysis of this model has shown that, for the above values of the interaction parameters, the model exhibits a low temperature ordered phase in which chains are tilted by about 27°. As the temperature is raised, Monte Carlo simulations show that the model exhibits a complex ripple phase with two typical wavelengths of about 160 Å and 220 Å (15, 16). Snapshots of the computer-generated ripples are very similar in appearance to scanning tunneling microscopy images (19). It must be pointed out that, due to the cosine term in Eq. 1, it is necessary to restrict differences in height of neighboring lipids ($\Delta n \leq 2$) to avoid unwanted periodicities in the interaction function. If this restriction is not enforced, the ripple phase is metastable relative to a flat bilayer phase with antiferromagnetic ordering in the head group variable (16). The cosine terms in Eq. 1 are a result of the mapping process, which is not unique in its nature. However, while the functional form of the mapping is not unique, any Hamiltonian which is faithful to the pre-calculated interactions must necessar-

TABLE 1 Number of peaks (of amplitude $\Delta n \geq 2$) in simulation cell for various values of $J_4$ and cholesterol content ($X_C$)

| $X_C$ | 0% | 2% | 7% | 10% |
|---|---|---|---|---|
| $J_4 = 0.1$ | 7 | 7 | 4 | 1 |
| $J_4 = 0.5$ | 7 | 7 | 5 | 1 |
| $J_4 = 1.5$ | 7 | 7 | | 1 |

$J_4$ is expressed in units of $J_0$.

ily have the low temperature phase sequence described above.

## Extension to Include Cholesterol

The PS2 model is extended to include cholesterol primarily by changing the model from a spin one-half to a spin one model. That is, the $\sigma$ variable, previously restricted to the values $\pm 1$, now is allowed to also have the value 0. The interpretation for lipid–cholesterol modeling is that a site at which $\sigma_{i,j} = 0$ is occupied by a cholesterol, while a site at which $\sigma = \pm 1$ is occupied by a L-shaped lipid, exactly as in the original model. Both lipid and cholesterol sites still require the state variable $n_{i,j}$ in addition to the spin variable for full specification.

An additional term must be added to Eq. 1, representing the interaction between cholesterol and lipid molecules or between pairs of cholesterol molecules on neighboring sites of the lattice. To gain some guidance for the nature of this term, interaction energies were calculated for a lipid molecule (DMPC) and an adjacent cholesterol molecule. This calculation is far less certain than the lipid–lipid calculations carried out earlier (14) because there are a very large number of ways two such dissimilar molecules may align themselves. As in previous work (14), 6–12 interactions were assumed between all non-hydrogen atoms of both molecules and 6–12 parameters determined for hydrocarbon by Jorgensen and co-workers (20) were used. The 6–12 parameters for benzene were used for the ring carbons in cholesterol (20).

Fig. 1 shows four typical lipid-cholesterol configurations and the associated interaction energies. It appears from our sampling of configurations that the minimum interaction energy is achieved when the chain of the cholesterol is near one of the lipid chains. In all cases interactions are weaker than the lipid–lipid interactions calculated earlier. The lipid–cholesterol calculations were done using DMPC rather than DPPC. But the addition of two carbons per chain will only make a small difference, because cholesterol is about the same length as the hydrophobic portion of DMPC. Additional close contact with the extra carbons on DPPC is not likely. Lipid–cholesterol interactions are weaker than lipid–lipid interactions because the molecules are not similar in steric shape, and thus cannot pack efficiently.

Guided by the energy calculations we have added the following term to the PS2 Hamiltonian:

$$\mathcal{H} = \mathcal{H}_{PS2} + \sum_{i}^{N} \sum_{j}^{N} J_4 x_{i,j;i+1,j} \qquad (2)$$

where $x_{i,j;i+1,j}$ is defined by:

- $x_{i,j;i+1,j} = 0$ if sites $[i,j]$ and $[i+1,j]$ both contain lipids or both contain cholesterol.
- $x_{i,j;i+1,j} = 1$ if site $[i,j]$ or $[i+1,j]$ contains a lipid and the other site contains a cholesterol, and the lipid head group points toward the cholesterol.
- $x_{i,j;i+1,j} = 2$ if site $[i,j]$ or $[i+1,j]$ contains a lipid and the other site contains a cholesterol, and the lipid head group points away from the cholesterol.

Because there is uncertainty in the optimal values of the lipid-cholesterol interaction strength, there is also uncertainty in the value to assign $J_4$. Note, however, that any value of $J_4 > 0$ leads to a weaker interaction between lipid and cholesterol, whenever $x > 0$. Given the functional nature of Eq. 1 the most reasonable values for $J_4$ are around 1. For $J_4 < 0.2$ lipid-cholesterol energies are only slightly less than lipid–lipid energies, while for $J_4 > 1.5$ the energies of certain lipid–cholesterol configurations are unrealistically large (repulsive). The interaction between lipid and cholesterol is slightly stronger when the lipid head group points toward the cholesterol (cholesterol $x = 1$), because this brings the head group closer to the cholesterol without producing steric overlap. Eq. 2 produces a strong attractive interaction energy between neighboring pairs of cholesterol molecules at the same height.

## Methods

The properties of the model have been determined by Monte Carlo simulation. The Monte Carlo (MC) procedure is the same as we used to analyze the spin one-half PS2 model for lipid–lipid interactions and moves. Lattice sites were selected randomly and, when a site occupied by a lipid was visited the spin variable was flipped and the height variable was changed by $\pm 1$ or 0, based on a random number. In order to study the behavior of the model at fixed cholesterol concentration, the total number of spin 0 molecules was held fixed. Initially the cholesterol sites were distributed randomly throughout the lattice. When a cholesterol (spin 0) site was visited in the

TABLE 2 Number of peaks in simulation cell vs. peak separation at four values of cholesterol concentration with $J_4$ = 1.45 kcal/mol = (.1066$J_0$)

| $X_C$ | 0% | 2% | 7% | 10% |
|---|---|---|---|---|
| <90 Å | 0 | 1 | 0 | 0 |
| 100–140 Å | 0 | 2 | 0 | 0 |
| 150–180 Å | 5 | 1 | 1 | 0 |
| 190–220 Å | 1 | 1 | 0 | 0 |
| >220 Å | 1 | 2 | 3 | 1 |
| TOTAL PEAKS | 7 | 7 | 4 | 1 |

MC walk, either the height of the cholesterol was changed by 0 or ±1, or an attempt was made to hop this molecule to a nearest neighbor site occupied by a lipid molecule. The hop consisted of an exchange of position with a lipid, if a near neighbor site occupied by a lipid existed.

The MC walk was carried out for the most part on 128 × 32 lattices, with the long direction along the axis of anisotropy (the axis for the head group orientation). As in earlier studies (16) of the spin one-half model, a simulated annealing procedure was followed, starting at $k_BT/J_0 = 1$ and proceeding to $k_BT/J_0 = 0.2$ in steps of 0.1. At each temperature 50,000 MC steps per site were run for equilibration followed by another 50,000 steps for averaging. This represents a considerable increase in the number of MC steps per site over earlier simulations (16), and the result is the ripples are considerably better defined at the lowest temperatures. A few MC runs were done on 256 × 32 lattices with 100,000 MC steps per site for averaging to check for size and run length effects. We found no discernible difference, so all results reported here are for 128 × 32 lattices, with the number of MC steps/site as given above.

## RESULTS

Since the configurations of the model become "locked in" after the annealing procedure, the ripple structure predicted by the model may equivalently be obtained from MC averages or from the final configuration. It is not possible to study dynamically changing ripples in these simulations because of the large-scale cooperative structural changes that would be required.

The principal result to emerge from the MC simulations is that the cholesterol molecules induce linear regions in the lattice which are flat and which lie at the ripple peaks or troughs. With increasing cholesterol content the flat regions expand, effectively pushing the ripples apart. This is in good accord with experimental observations (4–6).

Fig. 2 shows snapshots of ripple phases at $k_BT/J_0 = 0.2$ and $J_4 = 0.1066J_0 = 1.45$ kcal/mol for several cholesterol concentrations. The increase in the spacing of the ripples with increasing cholesterol concentration is clearly evident in this Figure. The flat areas consist of cholesterol molecules mixed with lipids with antiferromagnetic head group ordering. At higher cholesterol concentrations (≥15%) cholesterol molecules tend to aggregate. Fig. 3 is a series of density plots of the spin ordering corresponding to the cholesterol concentrations of Fig. 2. In all cases nearly all cholesterol molecules, which appear as dotted rectangles in Fig. 3, lie in the flat areas between the ripples. In Fig. 3 *d*, for which the cholesterol concentration is highest (10%), clustering of cholesterol molecules can be seen. This clustering is energetically favored in the model as cholesterol pairs with $\Delta n = 0$ are given a large negative interaction energy by the Hamiltonian Eq. 1.

Numerical information on the ripple repeat distances is given in Tables 1 and 2. Table 1 shows that the structure of the ripple phase depends only weakly on $J_4$, within the range of values of this parameter which are consistent with calculated intermolecular energies. Table 2 shows the distribution of ripple spacings for different cholesterol concentrations at $J_4 = 1.45$ kcal/mol. In the model, distances in ångströms are estimated as 10 times the number of lattice spacings, supposing that the lateral size of a lipid measured across both chains is about 10 Å.

The data in Table 2 may be compared with histograms of ripple repeat distance versus cholesterol concentration measured from freeze-fracture micrographs (5). At 0% cholesterol the theoretical model has a primary ripple spacing between 150 and 180 Å, with the greatest number of ripples having a 160 Å peak-to-peak distance. Other ripples occur with repeat distances of 200 and 250 Å in the model. In the freeze-fracture micrographs two populations of ripples are found, one with repeat spacings centered at about 130 Å and a much smaller population with a 240–280 Å repeat. At 2% cholesterol concentration the simulation cell for the model still contains seven ripples, but the distribution has shifted so that there are more flat areas between peaks. At 7% cholesterol concentration there are only five ripples in the simulation cell and the distribution has shifted more to larger repeat distance. Freeze-fracture micrographs at 5% cholesterol concentration show a peak in the ripple repeat distance of about 160–180 Å. At 10% cholesterol the model simulation cell contains only one ripple so the repeat distance is greater than 256 Å (twice the lattice size). The freeze fracture data show a repeat distance distribution which peaks at about 240 Å. At cholesterol concentrations greater than 10% the model simulations generally show one or no peaks, so that the ripple spacing is >256 Å. The freeze fracture data indicate a ripple spacing distribution with a maximum at over 400 Å at 15% cholesterol concentration.

## DISCUSSION

A critical test of any theoretical model is its ability to independently predict properties of the system under study. The extension of the spin one-half PS2 model to include cholesterol was an effort to perform such a test on this model. The inclusion of cholesterol was done by adding a third "spin" state to each site of the model lattice, so that $\sigma = 0$ at a site means the site is occupied by a cholesterol molecule rather than a phospholipid. Since cholesterol–lipid interaction energies were determined to be weaker than lipid–lipid interaction energies, it was also necessary to modify the model Hamiltonian. This was done in a very simple manner, involving only one additional interaction term in the Hamiltonian which incorporated energies for lipid–cholesterol pairs, and cholesterol-cholesterol pairs. Although the energies for

these pairs could not be calculated with the same precision as was possible for lipid–lipid pairs (14), the predicted properties of the model did not strongly depend on the value of $J_4$, the parameter which characterized these interactions, within the range considered.

The fact that these straightforward extensions to the model lead to predicted ripple structures which are in close accord with experiment indicates that the model contains the critical aspects of real systems which drive the ripple phase. As was mentioned in the Introduction, the PS2 model and the present extension are very simple, and omit or oversimplify several properties of lipid bilayers in their low temperature phases. The success of the model in predicting the effect of cholesterol on the ripple spacings, and the distribution of cholesterol within the $P_{\beta'}$ phase, suggest that the omissions are not major contributors to the physical mechanisms responsible for this phase.

There are several limitations to the model described here. The ripple spacings appear to be consistently somewhat larger than experimental data. Allowing headgroups only two orientations is overly restrictive. The model does not exhibit a chain melting phase transition. The temperature range at which the ripples occur appears to be too low (however because it is impossible to observe a direct transition from $P_{\beta'}$ to $L_{\beta'}$ phases in MC simulations, the exact location of this transition can only be estimated from mean field analysis on models with no height restrictions [16]). Clustering between pairs of cholesterol molecules may be overemphasized by the fact that Eq. 1 assigns an energy to pairs of cholesterols which is slightly stronger than the energy for the closest packed lipid pair (although clustering is not important for low cholesterol concentrations and is not a factor in the location of the cholesterols in the lattice).

The simplicity of this present model is an advantage in that the specific interactions responsible for the observed properties are clear. Cholesterol breaks up the ripples in the $P_{\beta'}$ phase by inducing defects in the regular lipid packing scheme associated with ripples in the model. Lipid–lipid interactions in the model only marginally favor ripple-like packing over flat packing. In fact, ripples occur because of a competition between these two packing schemes (15, 16). Introduction of cholesterol tips the balance in favor of flat chain packing in a neighborhood of each cholesterol site.

We thank Professor X. Xie for allowing us to run many of the simulations on an IBM RISC/6000 workstation in his laboratory, and Professor J. H. H. Perk for helpful discussions.

*Received for publication 29 September 1992 and in final form 28 December 1992.*

## REFERENCES

1. Presti, F. T. 1985. The role of cholesterol in membrane fluidity. In Membrane Fluidity in Biology. Vol. 4. Cellular Aspects, R. C. Aloia and J. M. Boggs, editors. Academic Press, New York. 97–146.
2. Lipid-cholesterol phase diagrams: Theoretical and numerical aspects. 1992. *In Cholesterol and Model Membranes.* L. Finegold, editor. CRC Press, Boca Raton, FL. 1992.
3. Vist, M. R., and J. H. Davis. 1990. Phase equilibria of cholesterol–Dipalmitoylphosphatidylcholine mixtures: $^2$H nuclear magnetic resonance and differential scanning calorimetry. *Biochemistry.* 29:451–464.
4. Copeland, B. R. and H. M. McConnell. 1980. The rippled structure in bilayer membranes of phosphatidylcholine and binary mixtures of phosphatidylcholine and cholesterol. *Biochim. Biophys. Acta.* 599:95–109.
5. Hicks, A., M. Dinda, and M. A. Singer. 1987. The ripple phase of phosphatidylcholines: Effect of chain length and cholesterol. *Biochim. Biophys. Acta.* 903:177.
6. Mortensen, K., W. Pfeiffer, E. Sackmann, and W. Knoll. 1988. Structural properties of a phosphatidylcholine-cholesterol system as studied by small angle neutron scattering: Ripple structure and phase diagram. *Biochim. Biophys. Acta.* 945:221–245.
7. Schneider, M. B., W. K. Chan, and W. W. Webb. 1983. Fast diffusion along defects and corrugations in phospholipid $P_{\beta'}$ Liquid Crystals. *Biophys. J.* 43:157–165.
8. Scott, H. L., and W. S. McCullough. 1991. Theories of the modulated ripple phase of lipid bilayers. *Int. J. Mod. Phys. B.* 5:2479–2497.
9. S. Doniach. A thermodynamic model for the monoclinic (ripple) phase of hydrated phospholipid bilayers. 1979. *J. Chem. Phys.* 70:4587–4596.
10. Marder, M., H. L. Frisch, J. S. Langer, and H. M. McConnell. 1984. Theory of the intermediate rippled phase of phospholipid bilayers. *Proc. Natl. Acad. Sci.* USA. 81:6559–6561.
11. Carlson, J. M., and J. Sethna. 1987. Theory of the ripple phase in hydrated phospholipid bilayers. *Phys. Rev. A* 36:3359–3374.
12. Goldstein, R., and S. Leibler. 1988. Model for lamellar phases of interacting lipid membranes. *Phys. Rev. Lett.* 61:2213–2215.
13. Cevc, G., 1991. Polymorphism of the bilayer membranes in the ordered phase and the molecular origin of the lipid pretransition and rippled lamellae. *Biochim. Biophys. Acta.* 1062:59–69.
14. Scott, H. L., and P. A. Pearce. 1989. Calculation of intermolecular interaction strengths in the $P_{\beta'}$ phase in lipid bilayers. *Biophys. J.* 55:339–345.
15. McCullough, W. S., and H. L. Scott. 1990. Statistical mechanical theory of the ripple phase of lipid bilayers. *Phys. Rev. Lett.* 65:931–934.
16. McCullough, W. S., J. H. H. Perk, and H. L. Scott. 1990. Analysis of a model for the ripple phase of lipid bilayers. *J. Chem. Phys.* 93:6070–6080.
17. Georgallas, A., and M. J. Zuckerman. 1986. Lipid vertical motion and related steric effects in bilayer membranes. *Eur. J. Biophys.* 14:53–61.
18. Hauser, H., I. Pascher, R. H. Pearson, and S. Sundell. 1981. Preferred conformation and molecular packing of phosphatidylethanolamine and phosphatidylcholine. *Biochim. Biophys. Acta.* 650:21–51.
19. Zasadzinski, J. A. N., J. Schneir, J. Gurley, V. Elings, and P. K. Hansma. 1988. Scanning tunneling microscopy of freeze-fracture replicas of biomembranes. *Science (Wash. DC).* 239:1013–1014.
20. Jorgensen, W. L., J. D. Madura, and C. J. Swendsen. 1984. Optimized intermolecular potential functions for liquid hydrocarbons. *J. Am. Chem. Soc.* 106:6638–6646.